



UNIVERSITY OF LEEDS

This is a repository copy of *Advancing In-Pipe Robot Communication with High-Speed OWC Transceiver Front-End Circuit: Experimental Insights and Prospects*.

White Rose Research Online URL for this paper:

<https://eprints.whiterose.ac.uk/218080/>

Version: Accepted Version

---

**Proceedings Paper:**

Boonlom, K., Khonrang, J., Rungrangsilp, S. et al. (3 more authors) (2024) Advancing In-Pipe Robot Communication with High-Speed OWC Transceiver Front-End Circuit: Experimental Insights and Prospects. In: 2024 21st International Conference on Electrical Engineering/Electronics, Computer, Telecommunications and Information Technology (ECTI-CON). 2024 21st International Conference on Electrical Engineering/Electronics, Computer, Telecommunications and Information Technology (ECTI-CON), 27-30 May 2024, Khon Kaen, Thailand. IEEE ISBN 979-8-3503-8156-6

<https://doi.org/10.1109/ecti-con60892.2024.10595010>

---

© 2024 IEEE. Personal use of this material is permitted. Permission from IEEE must be obtained for all other uses, in any current or future media, including reprinting/republishing this material for advertising or promotional purposes, creating new collective works, for resale or redistribution to servers or lists, or reuse of any copyrighted component of this work in other works.

**Reuse**

Items deposited in White Rose Research Online are protected by copyright, with all rights reserved unless indicated otherwise. They may be downloaded and/or printed for private study, or other acts as permitted by national copyright laws. The publisher or other rights holders may allow further reproduction and re-use of the full text version. This is indicated by the licence information on the White Rose Research Online record for the item.

**Takedown**

If you consider content in White Rose Research Online to be in breach of UK law, please notify us by emailing [eprints@whiterose.ac.uk](mailto:eprints@whiterose.ac.uk) including the URL of the record and the reason for the withdrawal request.



[eprints@whiterose.ac.uk](mailto:eprints@whiterose.ac.uk)  
<https://eprints.whiterose.ac.uk/>

# Advancing In-Pipe Robot Communication with High-Speed OWC Transceiver Front-End Circuit: Experimental Insights and Prospects

Kamol Boonlom  
School of Electronic and Electrical  
Engineering  
University of Leeds  
Leeds, United Kingdom  
elkbo@leeds.ac.uk

Jarun Khonrang  
Faculty of Industrial Technology  
Chiang Rai Rajabhat University  
Chiangrai, Thailand  
Jarun.kho@crju.ac.th

Suppat Rungraungsilp  
School of Electronic and Electrical  
Engineering  
University of Leeds  
Leeds, United Kingdom  
elsru@leeds.ac.uk

Tim Amsdon  
School of Electronic and Electrical  
Engineering  
University of Leeds  
Leeds, United Kingdom  
T.J.Amsdon@leeds.ac.uk

Ian Robertson  
School of Electronic and Electrical  
Engineering  
University of Leeds  
Leeds, United Kingdom  
I.D.Robertson@leeds.ac.uk

Nutapong Somjit  
School of Electronic and Electrical  
Engineering  
University of Leeds  
Leeds, United Kingdom  
N.Somjit@leeds.ac.uk

**Abstract**— This paper presents the design and experimentation of a high-speed optical wireless communication front-end transceiver circuit tailored for in-pipe robot communication applications. The design process encompasses circuit simulation using the TINA-TI simulation program, PCB fabrication, and subsequent testing within a plastic pipe environment. Experimental findings indicate a system frequency bandwidth of 19.53 MHz for analog modulation at an HB-LED wavelength of 475nm and 300 mA, with an observed attenuation rate of 0.24 dB/cm within the in-pipe setting. Digital modulation experiments yield peak data rates exceeding 50 Mbps for OOK modulation and over 20 Mbps for the PRBS signal. These results hold significant promise for the advancement of optical wireless communication applications in robotics and future 6G communications.

**Keywords**— **Optical wireless communication, Inspection robots, In-pipe communication.**

## I. INTRODUCTION

Currently, robot technology has taken on more roles and duties in place of humans, especially in dangerous and risky areas, and areas that are difficult to access. This can be clearly seen from a group of researchers who study and develop robots that survey water pipes by allowing the robot to explore and collect information about the environment in pipes that are buried underground [1], etc.

Wireless communication technology is essential for underground in-pipe robots as it enables seamless communication between robots and users, as well as between different robots. The use of wireless systems is primarily driven by their ability to cover long distances and their cost-effectiveness. There are three commonly used forms of wireless communication: acoustic waves, radio waves, and optical wireless communication [1].

Acoustic wireless communication offers efficient underwater transmission, low power usage, compatibility with existing infrastructure, and reduced electromagnetic interference [2]. Its ability to propagate over long distances and penetrate obstacles makes it ideal for underwater applications like oceanography and underwater navigation.

However, acoustic wireless communication suffers from lower data rates, susceptibility to noise and interference, limited bandwidth, higher latency [3], and environmental sensitivity compared to RF communication.

While RF communication provides benefits such as higher data rates, wider bandwidth, lower susceptibility to environmental factors, longer range, and more reliable performance, its use in underground pipes is hindered by challenges like signal attenuation, interference, multipath propagation, limited penetration, and increased power consumption. These factors can diminish signal quality, restrict communication range, and undermine reliability in subterranean settings [4].

Optical wireless communication systems (OWC) represent a cornerstone technology in 6G communication. They offer substantially higher bandwidth capabilities compared to RF systems, facilitating faster data transmission rates, making them ideal for applications demanding high data throughput [5], [14]–[16]. Optical signals are impervious to electromagnetic interference, enhancing signal reliability in environments with electronic devices or electromagnetic radiation sources. Additionally, optical communication systems generally exhibit lower latency than RF systems, making them well-suited for real-time data transmission needs in scenarios like high-frequency trading or interactive gaming [6], [7].

Overall, optical wireless communication offers numerous advantages compared to both acoustic and RF communication technologies. It provides higher bandwidth and data rates, lower susceptibility to interference, enhanced security due to the directional nature of light, lower latency, and freedom from spectrum congestion [9]–[11]. Additionally, optical wireless communication is more suitable for environments where RF signals may face challenges, such as underwater or in areas with high electromagnetic interference [8].

The front-end part of optical wireless communication serves as the interface connecting the optical transmitter and receiver components to the rest of the communication system [12], [13]. The main purpose of this device is to effectively convert electrical signals into optical signals for transmission and vice versa. These tasks involve data modulation and

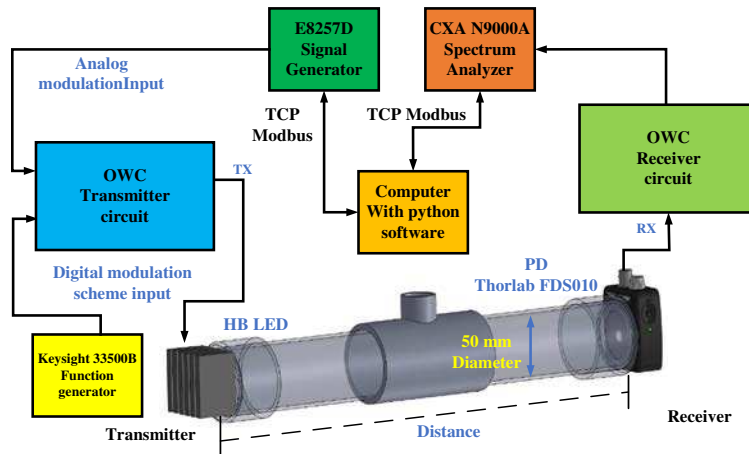


Fig. 1. depicts the experimental setup of the OWC front-end utilized in the experiment.

demodulation, signal amplification, noise filtering, and the management of transmission and reception. In addition, it may contain signal conditioning components, such as equalization or amplification, to enhance the performance of the communication link [16].

The primary objective of this study is to develop a specialized front-end circuit for optical wireless communication that can be seamlessly integrated with a pipe inspection robot. The experimental results will demonstrate the data transmission performance within a plastic pipe with a diameter of 50 mm, which encompasses both analog and digital formats.

The design process of the optical wireless communication front-end circuit is thorough, encompassing simulation, fabrication, and rigorous testing. The performance of the communication system was evaluated by simulating it using TINA-TI Simulation and then fabricating the circuit. The circuit's effectiveness was evaluated through actual testing conducted on a small plastic pipe measuring 50mm in diameter, yielding valuable insights. The circuit's performance and reliability were thoroughly evaluated in practical scenarios using both analog and digital modulation schemes during testing. This comprehensive approach guarantees the creation of a strong and effective optical wireless communication system that is suitable for a wide range of applications.

## II. OWC FRONT-END CIRCUITS DESIGN AND SIMULATION

In this section, we explore the design intricacies of the optical wireless communication (OWC) front-end circuit, encompassing both the OWC transmitter and receiver. Simulation tasks are seamlessly facilitated through the utilization of the TINA-TI Simulation software.

### A. OWC transmitter design

Fig. 2 depicts the operational schematic of the OWC transmitter circuit. It showcases the utilization of high-speed MOSFET drivers, which are the ISL55110, to drive the input signal for amplification through the IRF7103. The amplified signal is then directed towards powering a 1W LED that emits light at a wavelength of 475nm. The process entails modulating the input signal with the carrier signal of the LED while maintaining a constant current of 300 mA for optimal LED performance.

Fig. 3 illustrates the simulation outcomes of the OWC transmitter circuit. The LED operates with a consistent current of 300 mA and is modulated using a pulse input signal. This modulation approach enables higher data transmission speeds compared to using on-off modulation, which can introduce signal delays [16].

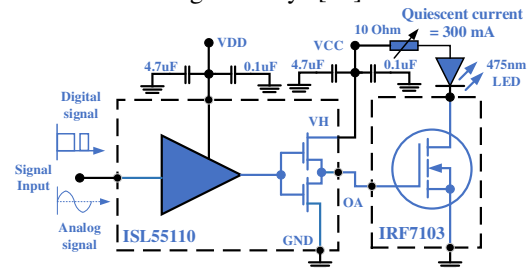


Fig. 2. Schematic diagram of the OWC transmitter for robot inspection.

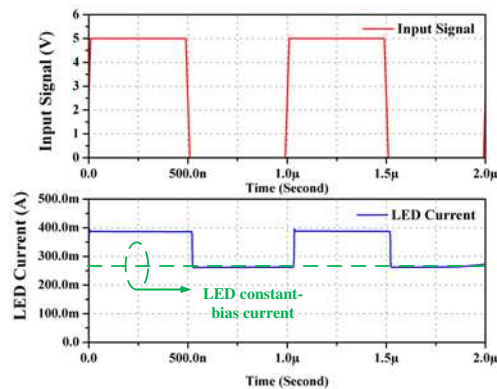


Fig. 3. Schematic diagram of the OWC transmitter for robot inspection.

### B. OWC receiver design

Fig. 4 depicts a schematic diagram of the OWC receiver circuit, comprising four analog sub-circuits: the trans-impedance amplifier, equalizer, post-amplifier, and pre-detection filter. The four subsystems are interconnected in a cascade and are designed to be used on the same printed circuit board (PCB). The circuit functions using two power supply rails: +12V and -12V. The -12V supply is used to apply reverse bias (VR) to the photodiode (PD). The +12V supply powers the linear LED regulator, which generates the

necessary +5 V and -5 V voltage levels for the operational amplifier functions.

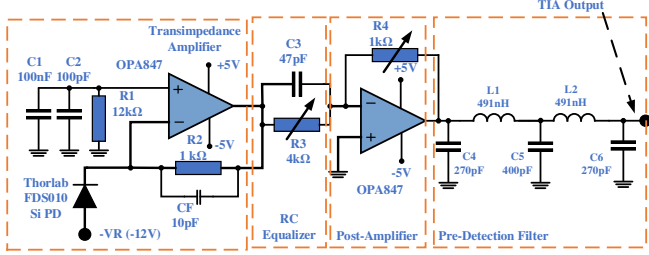


Fig. 4. Schematic diagram of the OWC receiver for robot inspection.

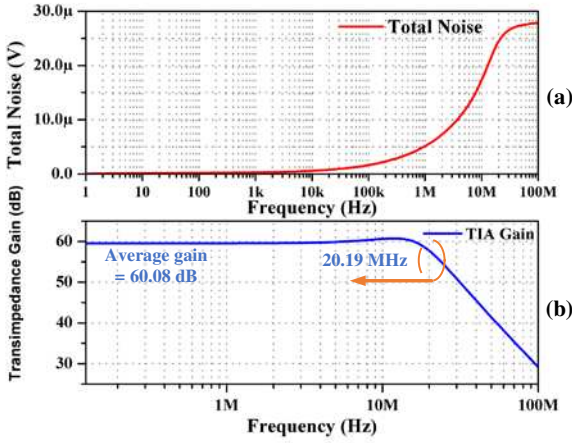


Fig. 5. Simulation results for the gain and total noise of the TIA are presented.

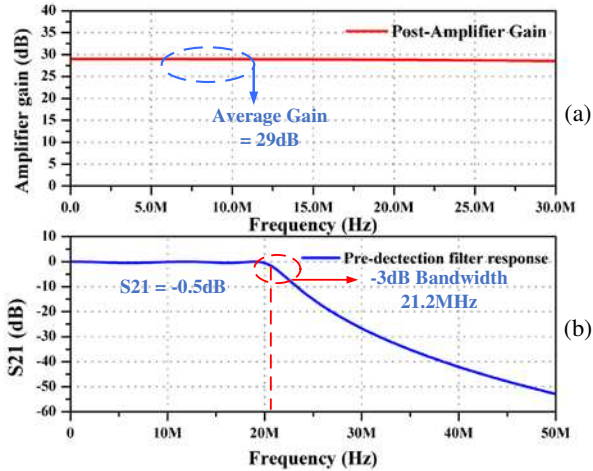


Fig. 6. Simulation results for the post-amplifier and filter response.

The simulation results for the trans-impedance amplifier are shown in Fig. 5(b). The average gain value within the operational range is 60.08 dB, with a maximum frequency of 20.19 MHz. Furthermore, fig. 5(a) illustrates the simulation results, showing a noise value of 24.07  $\mu$ V at a frequency of 20 MHz. Fig. 6(a) shows the simulation results for the post-amplifier circuits, demonstrating a gain of 29 dB across a frequency bandwidth of more than 20 MHz. Fig. 6(b) displays the frequency response of the circuit, covering a range of 0 to 20 MHz. In addition, the simulation results show that the pre-detection filter has an S21 value of -0.5 dB and a -3 dB frequency bandwidth of 21.2 MHz.

### C. Window comparator module

Fig. 7 illustrates the schematic diagram of the window comparator module, which comprises two analog subsystems: the window comparator and the differential PECL to TTL logic translator. The output signal is digitized by applying a composite signal to an AC coupling and a 0.5 V DC offset circuit, which centers the composite signal within the range of 0 V to 1 V of the window comparator. This comparator consists of IC1 and a dual comparator, IC2.

The pulse threshold detection voltage ( $V_{REF+}$ ) is set at 0.75 V. Afterward, the differential PECL outputs of the window comparators are directed to the PECL to TTL translator IC2.

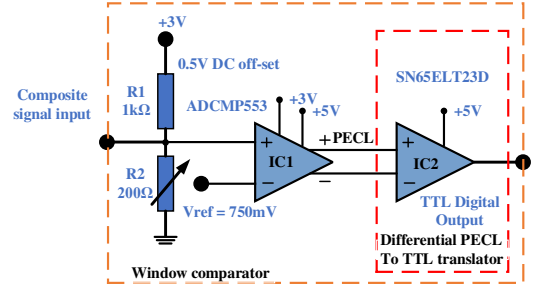


Fig. 7. Schematic diagram of the window comparator circuit.

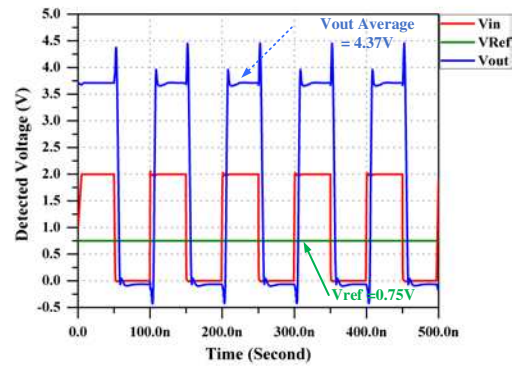


Fig. 8. Simulation results for the window comparator circuit.

The simulation outcomes of the window comparator circuit are shown in Fig. 8. The output signal shows an average level of 4.37 volts, although there is a small phase difference when compared to the input signal. The observed deviation is a result of signal delays caused by the cascaded amplifier equipment.

### III. IN-PIPE EXPERIMENTAL SETUP

In this section, we will explore the process of establishing an experiment to assess optical wireless communication in a plastic pipe environment. The objective is to evaluate the influence of pipe conditions on different parameters and the effectiveness of data transmission facilitated by the designed circuit.

Fig. 1 depicts the experimental setup devised for testing data transmission through a plastic pipe. The pipe measures 50 mm in diameter and spans a length of 350 mm. The experiment utilizes two modulation schemes: analog signal modulation and digital modulation. The experimental analog modulation scheme utilizes a sine wave signal generated by the RF signal generator E8257D. The frequency range of this spans from 125 kHz to 30 MHz, while the amplitude is set at 10 dBm. The LED specified for this particular application is

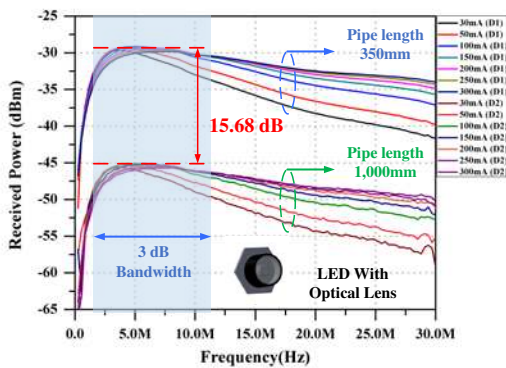
the Osram 720-LBCRBPA6186, which operates at a wavelength of 475nm. The decision to employ blue LEDs is driven by their wider bandwidth, which allows for faster data transmission at the receiver end. The analog signal received by the receiver circuit is directed to the spectrum analyzer N9000A in the experimental setup. Afterwards, the data is captured and recorded on a computer using a Python program. This program allows for control of the two measuring instruments through the TCP Modbus protocol. A digital pseudorandom binary sequence (PRBS) signal is generated in the digital modulation scheme using an arbitrary function generator, such as the Keysight 33500B. The signal is subsequently modulated into the circuit of the LED transmitter. The signals on the receiver end are measured using a digital oscilloscope, which is the DXOX2024A, to record the data rate of the received data.

#### IV. IN-PIPE MEASUREMENT RESULTS

In this section, we will delve into the experimental results, specifically focusing on the frequency response of analog transmission within the plastic pipe as well as the observed attenuation in the connecting pipe. Examine and evaluate the frequency bandwidth of the system when utilizing an analog signal. The subsequent phase of testing involves examining the experimental outcomes of employing digital modulation. This includes evaluating the data rate achievable with the designed circuit within the pipeline data transmission environment, along with determining the modulation bandwidth utilized for digital modulation.

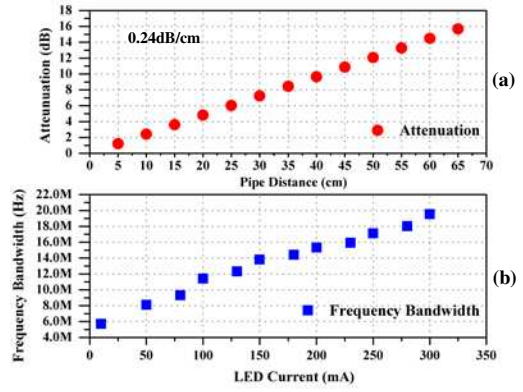
##### A. Analog modulation scheme response

Fig. 9 illustrates the frequency response of analog signal transmission within the in-pipe environment at distances of 350 mm and 1,000 mm. The experimental results, when normalized, reveal that increasing the bias current of the LED leads to an expansion in the frequency bandwidth (3 dB bandwidth). The measurement results indicate that the maximum frequency bandwidth, as depicted in Fig. 10 (b), reaches 19.53 MHz at an LED current of 300 mA.



**Fig. 9.** illustrates the frequency response of analog signal transmission.

Fig. 10 (a) illustrates the signal levels measured at various lengths of the plastic pipe, showcasing a decline in signal strength with increasing pipe length. The observed variation in signal levels across different pipe lengths amounted to 15.68 dB. Utilizing (1), the attenuation rate per unit length is computed at 0.24 dB/cm for a wavelength of 475 nm.



**Fig. 10** illustrates the attenuation value corresponding to each pipe length and the frequency bandwidth relative to the LED current.

$$PipeAtten (dB / cm) = \frac{10 \log \left[ \frac{D1_{Power}}{D2_{Power}} \right]}{P_L} \quad (1)$$

Where,  $D1_{Power}$  is the received power at a length of 350mm,  $D2_{Power}$  is the received power at a length of 1,000 mm, and  $P_L$  is the length difference of the plastic pipe equal to 650mm.

##### B. Digital modulation scheme response

In the digital modulation scheme experiment, two types of signals are utilized for modulation. Firstly, modulation with an on-off keying (OOK) is employed, where the duty cycle of the pulse signal is set at 50% with an amplitude equal to 5 V<sub>rms</sub>. The signal frequency is then varied from 100 kHz to 20 MHz.

Fig. 11(a) depicts the relationship between frequency bandwidth and output amplitude in the context of OOK signal modulation. In Fig. 11(b), it can be observed that as the frequency bandwidth increases, the output amplitude decreases, and the bit rate increases.

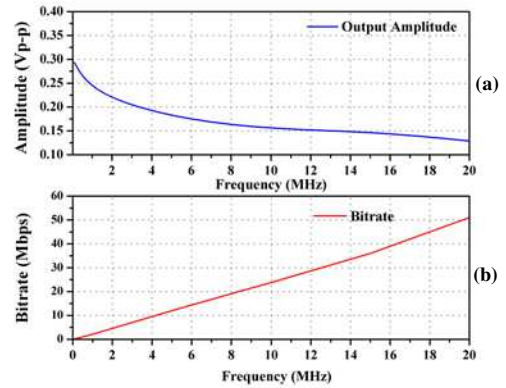


**Fig. 11.** shows the OOK modulation frequency bandwidth, bitrate, and output amplitude relationship.

Figs. 12(a)–(b) illustrate the correlation between bitrate, output amplitude, and frequency bandwidth in the context of the PRBS signal. It is important to note that as the bit rate increases, there is a corresponding rise in frequency bandwidth while the output voltage decreases.

Figs. 13 (a)–(f) illustrate the output signal obtained from the Transimpedance Amplifier (TIA) circuit of the receiver. As the transmission frequency increases, the

waveform of the signal undergoes changes due to the scattering effect within the pipe, resulting in a decrease in signal strength. For instance, at a frequency of 100 kHz, the signal amplitude measures 293 mVp-p, with a bit rate of 201 kbps. Conversely, at a frequency of 20 MHz, the signal level decreases to 129 mVp-p, with a bit rate of 51 Mbps.

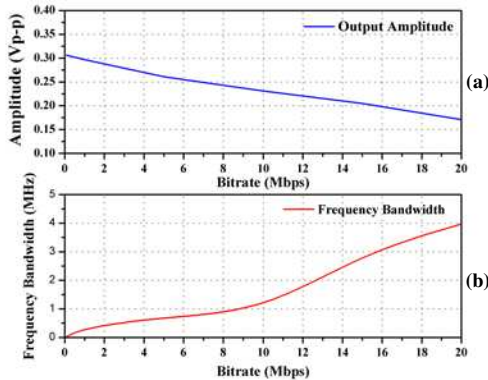


**Fig. 12.** shows the PRBS signal frequency bandwidth, bitrate, and output amplitude relationship.

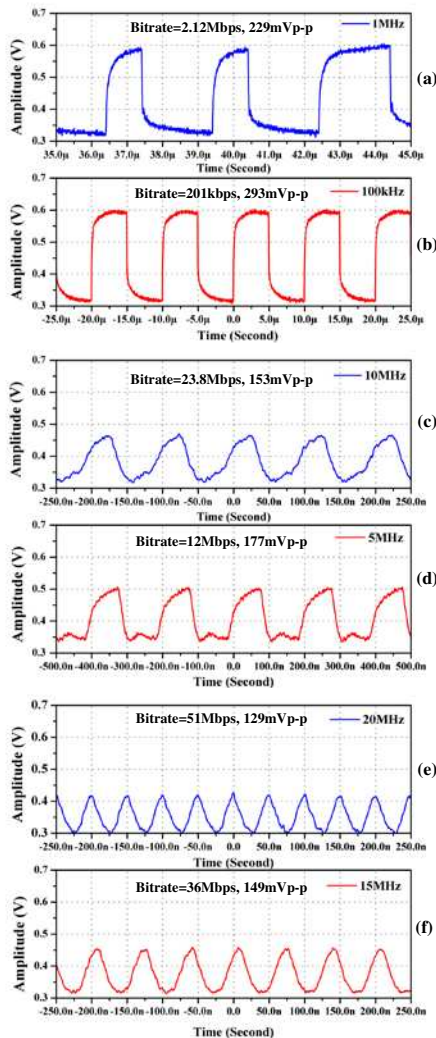


**Fig. 13.** illustrates the received output signal resulting from OOK modulation at the receiver.

In the modulation using a PRBS signal, the investigation aimed to assess the frequency bandwidth utilization by progressively increasing the data bitrate from 100 kbps to 20 Mbps, as depicted in Figs. 14 (a)–(f).

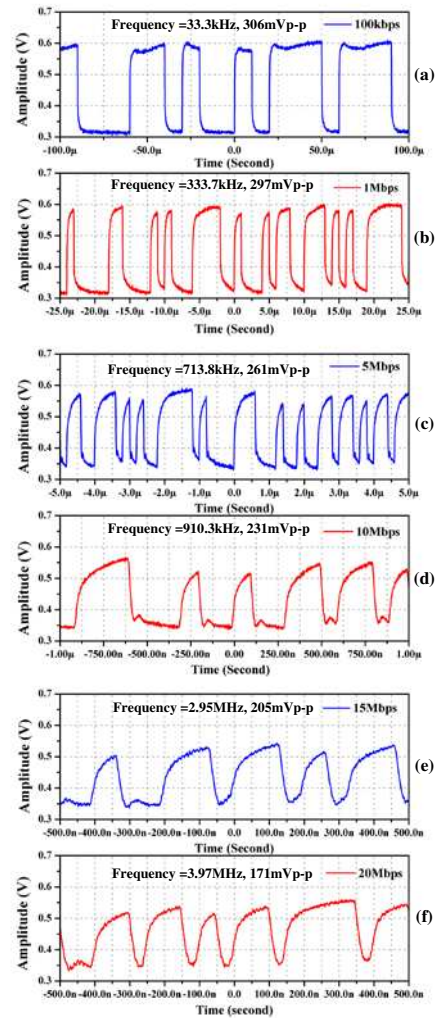


**Fig. 14.** illustrates the received output signal resulting from the PRBS signal at the receiver.

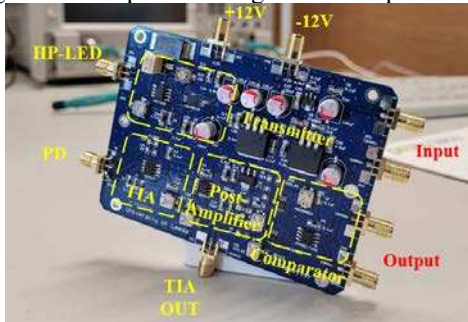
The results demonstrate a direct correlation between bitrate and frequency bandwidth, where higher bitrates correspond to increased bandwidth consumption. However, concurrently, there is a reduction in the received signal level with escalating bitrates. For instance, at a bitrate of 100 kbps, the frequency bandwidth measures 33.3 kHz with an amplitude of 306 mVp-p. Conversely, at a bitrate of 20 Mbps, the frequency bandwidth extends to 3.97 MHz, with an amplitude of 171 mVp-p.

Fig. 15 displays the fabrication of the OWC front-end circuit, while Fig. 16 showcases the test setup specifically designed to evaluate optical wireless communication in an in-pipe environment.

This study elucidates the intricate interplay between modulation schemes, signal frequencies, and pipe lengths that critically affect the performance of OWC systems within pipe environments. By optimizing the LED bias current and carefully selecting modulation parameters, enhancements in data transmission capabilities are achievable, along with notable reductions in signal attenuation.

The research successfully demonstrates the potential of OWC systems to achieve data transmission speeds of up to 20 Mbps. However, this study's scope does not explicitly address the presence of an acceptable bit error rate (BER), despite its critical role in understanding the limits of data

transmission reliability. Future investigations are essential to quantify the BER further and to refine the system to balance speed and error rate effectively, ensuring robust and reliable communication in complex in-pipe settings. This groundwork lays the foundation for advancing OWC technology, particularly in enhancing in-pipe communication systems, where traditional methods may falter. Furthermore, studies have shown that the pipe's maximum distance is 1 meter. Nevertheless, when used at greater distances, it becomes necessary to augment the signal intensity. Increasing both the input and the gain of the optical receiver.



**Fig. 15.** displays the fabrication of OWC front-end transceiver circuits.

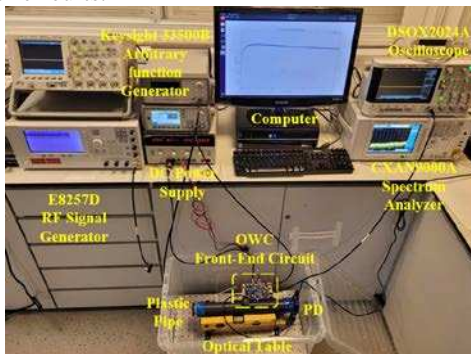


**Fig. 16.** An experimental test rig was implemented in the research.

## V. CONCLUSION

In conclusion, this study showcases the development and evaluation of a high-speed optical wireless communication front-end transceiver circuit tailored specifically for in-pipe robot communication scenarios. Through a comprehensive design process involving circuit simulation, fabrication, and testing, the performance of the system was thoroughly assessed within a plastic pipe environment. The test results show that the frequency range for analog modulation is quite large, at 19.53 MHz, and the attenuation rate in the in-pipe setting is 0.24 dB/cm. Additionally, digital modulation experiments yielded impressive peak data rates exceeding 50 Mbps for OOK modulation and over 20 Mbps with the PRBS signal. These findings underscore the potential of optical wireless communication technologies to enhance communication capabilities for robotic applications and pave the way for future advancements in 6G communications.

## Acknowledgements

This work is supported by the UK's Engineering and Physical Sciences Research Council (EPSRC) Programme

Grant EP/S016813/1 and a scholarship from Chiang Rai Rajabhat University, Thailand, number FF67-1-001.

## REFERENCES

- [1] Pipebots. (2023, November 3). Pipebots. <https://pipebots.ac.uk/>
- [2] J. W. Choi, A. V. Borkar, A. C. Singer and G. Chowdhary, "Broadband Acoustic Communication Aided Underwater Inertial Navigation System," in *IEEE Robotics and Automation Letters*, vol. 7, no. 2, pp. 5198-5205, April 2022, doi: 10.1109/LRA.2022.3154004.
- [3] Hawley, M. E. (1956, March 1). Acoustic Interference for Noise Control. *Noise Control*, 2(2), 61-94. <https://doi.org/10.1121/1.2369191>
- [4] H. Guo et al., "A Low-Cost Through-Metal Communication System for Sensors in Metallic Pipes," in *IEEE Sensors Journal*, vol. 23, no. 8, pp. 8952-8960, 15 April 2023, doi: 10.1109/JSEN.2023.3253663.
- [5] M. Alsabah et al., "6G Wireless Communications Networks: A Comprehensive Survey," in *IEEE Access*, vol. 9, pp. 148191-148243, 2021, doi: 10.1109/ACCESS.2021.3124812.
- [6] Lockwood, H., Wittke, J., & Ettenberg, M. (1976, January). LED for high data rate, optical communications. *Optics Communications*, 16(1), 193-196. [https://doi.org/10.1016/0030-4018\(76\)90083-3](https://doi.org/10.1016/0030-4018(76)90083-3)
- [7] Jahid, A., Alsharif, M. H., & Hall, T. J. (2022, April). A contemporary survey on free space optical communication: Potentials, technical challenges, recent advances and research direction. *Journal of Network and Computer Applications*, 200, 103311. <https://doi.org/10.1016/j.jnca.2021.103311>
- [8] H. Haas, J. Elmirghani, and I. White, "Optical wireless communication," *Philosophical Transactions of the Royal Society A: Mathematical, Physical and Engineering Sciences*, vol. 378, no. 2169, Apr. 2020.
- [9] Schirripa Spagnolo G, Cozzella L, Leccese F. Underwater Optical Wireless Communications: Overview. *Sensors (Basel)*. 2020 Apr 16;20(8):2261. doi: 10.3390/s20082261. PMID: 32316218; PMCID: PMC7219055.
- [10] Ke Wang, Tingting Song, Yitong Wang, Chengwei Fang, Jiayuan He, Ampalavanapillai Nirmalathas, Christina Lim, Elaine Wong, and Sithamparanathan Kandeepan, "Evolution of Short-Range Optical Wireless Communications," *J. Lightwave Technol.* 41, 1019-1040 (2023)
- [11] Chowdhury, M. Z., Hasan, M. K., Shahjalal, M., Hossain, M. T., & Jang, Y. M. (2020). Optical Wireless Hybrid Networks: Trends, Opportunities, Challenges, and Research Directions. *IEEE Communications Surveys & Tutorials*, 22(2), 930-966. <https://doi.org/10.1109/comst.2020.2966855>
- [12] K. Boonlom et al., "Active Pre-Equalizer for Broadband Optical Wireless Communication Integrated with RF Amplifier," 2022 Research, Invention, and Innovation Congress: Innovative Electricals and Electronics (RI2C), Bangkok, Thailand, 2022, pp. 251-254, doi: 10.1109/RI2C56397.2022.9910315.
- [13] K. Boonlom, R. Viratikul, I. D. Robertson, T. Amsdon, N. Chudpooi and N. Somjit, "Illumination and Bandwidth Control Circuit for LED Optical Wireless Transmitter Driver Integrated with Passive Second-Order Equaliser for Pipe Robot Application," 2023 Research, Invention, and Innovation Congress: Innovative Electricals and Electronics (RI2C), Bangkok, Thailand, 2023, pp. 1-5.
- [14] Khonrang, J., Somphruek, M., Duangnakhorn, P., Siri, A., & Boonlom, K. (2022, December 27). Experimental and Case studies of Longdistance Multi-hopping Data Transmission Techniques for Wildfire Sensors Using the LoRa-Based Mesh Sensor Network. *International Journal of Electronics and Telecommunications*, 419-424.
- [15] Binbin Hong, Naixing Feng, Jing Chen, Guo Ping Wang, Viktor Doychinov, Roland Clarke, John Cunningham, Ian Robertson, and Nutapong Somjit, "Substrate integrated Bragg waveguide: an octave-bandwidth single-mode hybrid transmission line for millimeter-wave applications," *Opt. Express* 28, 27903-27918 (2020)
- [16] Amsdon, Timothy J. and Martin J. N. Sibley. "Theoretical concepts and matlab modelling of VLC based MIMO systems." (2013).